# Theoretical studies of spin-dependent electrical transport through carbon nanotbes

S. Krompiewski

Institute of Molecular Physics, Polish Academy of Sciences, ul. M. Smoluchowskiego 17, 60179 Poznan, Poland

Abstract. Spin-dependent coherent quantum transport through carbon nanotubes (CNT) is studied theoretically within a tight-binding model and the Green's function partitioning technique. End-contacted metal/nanotube/metal systems are modelled and next studied in the magnetic context, i.e. either with ferromagnetic electrodes or at external magnetic elds. The former case shows that quite a substantial giant magnetoresistance (GMR) e ect occurs ( 20%) for disorder-free CNTs. Anderson-disorder averaged GMR, in turn, is positive and reduced down to several percent in the vicinity of the charge neutrality point. At parallel magnetic elds, characteristic Aharonov-Bohm-type oscillations are revealed with pronounced features due to a combined e ect of: length-to-perimeter ratio, unintentional electrode-induced doping, Zeeman splitting, and energy-level broadening. In particular, a CNT is predicted to lose its ability to serve as a magneto-electrical switch when its length and perimeter become comparable. In case of perpendicular geometry, there are conductance oscillations approaching asymptotically the upper theoretical limit to the conductance, $4e^2/h$. Moreover in the ballistic transport regime, initially the conductance increases only slightly with the magnetic eld or remains nearly constant because spin up- and spin down-contributions to the total magnetoresistance partially compensate each other.

PACS numbers: 81.07.De, 75.47.De, 75.47.Jn

## 1. Introduction

Recently a new field of electronics called spin electronics or just spintronics has been rapidly developing. In comparison with conventional electronics the most obvious advantage the spintronics offers is a possibility of controlling current flowing through mesoscopic or nanoscopic systems with magnetic field, by making use of the spin degree of freedom of electron. The well-known example illustrating this, is the famous giant magnetoresistance (GMR) effect, initially discovered in all-metal multilayers [1], and next also in all-semiconductor tunnel junctions [2], and molecular systems [3]. Here the main interest will be focused on a very peculiar class of the latter – namely carbon nanotubes (CNT) [4]. The GMR effect can only be observed when some parts of a circuit (usually electrodes) are ferromagnetic, then magnetic field polarizes them making thereby the electrical transport spin-dependent (see e.g [5, 6] for excellent state-of-the-art reviews). Quite interesting quantum effects do also appear in non-magnetic systems in the presence of external magnetic field. The carbon nanotube are quite exceptional in this context, as they may undergo magnetic field-induced major changes in their energy band structure, resulting even in turning a metallic CNT into a semiconductor or vice versa. This phenomenon, predicted theoretically [7, 9], has been recently confirmed experimentally, so it is clear now that axial magnetic field, if strong enough, may lead to successive opening and closing of an energy gap between the conduction and valence bands. Some of these phenomena occurring in CNTs, e.g the Aharonov-Bohm (AB) effect, as well as conductance oscillations in perpendicular magnetic field due to the Landau-like quantization will be also addressed in the sequel. It is noteworthy that very much like the GMR effect, believed to have practical applications in CNT-based spintronic devices, also the AB effect in nanotubes might be used to construct magneto-optical or magneto-electrical switches. One of the objectives of this study is to elucidate the importance of size effects directly related to miniaturization problems and the possibility of using tiny CNTs as elements of functional devices and interconnects in nanoelectronics. Ultra short CNTs, with comparable circumferences and lengths, have not yet been experimentally studied as far as their transport properties are concerned, in spite of the fact that some other ultra short molecular systems, including fullerene, were successfully electrically contacted and measured ([10], [11]). The shortest carbon nanotube segments operated with so far have been about 20 nm long [12]. Such segments may be created with an AFM tip in a double-buckle nanotube form.

The paper is organized as follows: In Sec. 2 the computational method based on a tight-binding model is shortly outlined. Sec. 3 is devoted to the GMR effect, whereas in the subsequent section (Sec. 4) the effect of magnetic field on electrical transport is discussed. Finally main results of the paper are summarized.

## 2. Methodology and Modelling

We use a tight-binding model for non-interacting -electrons within nanotubes and s-electrons in each of the two metal-electrodes. In the case of ferromagnetic electrodes the s-electron spin-split band is supposed to mimic d bands of real transition metals. The total Hamiltonian reads

$$H = \sum_{i;j;} t_{i;j} \, ji; \; ih \; ;jj + \sum_{i;} \; _{i;} \; ji; \; ih \; ;ij; \qquad (1)$$

where i and j run over the whole device (i.e the CNT itself and the electrodes), is the spin index, and $t_{i;j}$ and $_{i;}$ stand for the hopping integrals and the on-site potentials, respectively. This is an independent-electron model, applicable in the case of high-transparency contacts, and a relatively long mean free-path, i.e. when electrical transport can be regarded as quasi-ballistic ([13] – [16]).

Carbon nanotubes have been simulated by means of codes based on those of Ref. [9] (see Appendix therein). The model electrodes are fcc(1,1,1) leads in nite in all the 3 directions contacted to CNTs via a constriction composed of 2 nite atomic planes of each electrode. So the whole system (device) considered here is end-contacted, in contrast to other wide-spread geometries, like those of side-contact- and embedded-contact-schemes. The device has been relaxed in order to nd energetically favorable positions of interface atoms. The interface metal atoms have been modelled by spheres $d_M = 2.51$ A in diameter (this gure roughly ts to the most common metal electrodes). Carbon atoms in turn, have been represented by smaller spheres with diameter equal to $d_C = 1.421$ A. Using simple geometrical arguments it is assumed that interface CNT atoms tend to be as close as possible to their neighboring metal atoms (big spheres). So the Lennard-Jones potential (any other would also work) is simply $( =r)^{12} \quad ( =r)^6$ with a parameter $= (d_M + d_C)=2$ and an irrelevant pre-factor set to 1. Hereafter, the CNT together with the aforementioned extra atomic planes will be referred to as the extended molecule. The way the on-site ($_i$) potentials are determined is as follows. First the $_i$-s are set equal to those of separated components of the device, i.e. for CNTs $_i = 0$ (charge neutrality point), and for electrodes { to a certain nonzero-value chosen so as to give a required number of electrons per atom. In the ferromagnetic case spin-dependent on-site potentials must additionally give a required magnetic moment per atom. This has been implemented by making a rigid band (Stoner) splitting in the metal electrodes. The on-site potentials referring to intrinsically non-magnetic carbon atoms have not been split. Of course when the electrodes are magnetic (Sec. 3), self-consistent calculations result in inducing slight magnetic moments at interface carbon atoms. In the present model calculations an average number of electrons per metal atom is equal to n= 1 and its spin polarization, de ned as $P = 100(n_{\uparrow} \quad n_{\downarrow})=(n_{\uparrow} + n_{\downarrow})$, quals 50% . Second, an extra self-consistent potential has been added to diagonal matrix elements of the Hamiltonian referring to the extended molecule. At the rst step of the self-consistency loop a self-consistent potential is set 0, whereas during the next steps

it is modified so as to give no global charge excess on the extended molecule, with the total charge given by the trace of the density matrix $\hat{n}$ (Eq. 3, see below). This simple procedure makes it possible to line up the CNT and metal electron energy bands, and fix the position of the Fermi level, in particular. As an example, Fig. 1 shows the number of electrons per atom in a device composed of infinitely large electrodes (in the x, y, z directions, not shown) end-contacted via finite two-plane necks (A, B) to a (24,24)-CNT (region C). Figure 1 is a 1-d visualization of a 3-d system with atoms aligned as in a chain, so atoms labelled with consecutive numbers are usually not nearest neighbors. Abrupt charge changes visible in this figure in the A and B regions are due to edge atoms with reduced neighborhood, which do not contribute effectively to electron scattering. It is instructive to note that our simple model gives a qualitatively correct physical picture with strong oscillations in the number of electrons per atom in the vicinity of the interface which next get weakened and die down. It should be however made clear that a more direct way to align the Fermi levels, while dealing with real electrodes, would consist in taking into account work functions (WF) of involved materials (carbon vs. metal). In fact the work function of a CNT is usually supposed to be roughly equal to that of the graphite i.e. 4.5 eV (as a matter of fact it is however chirality-

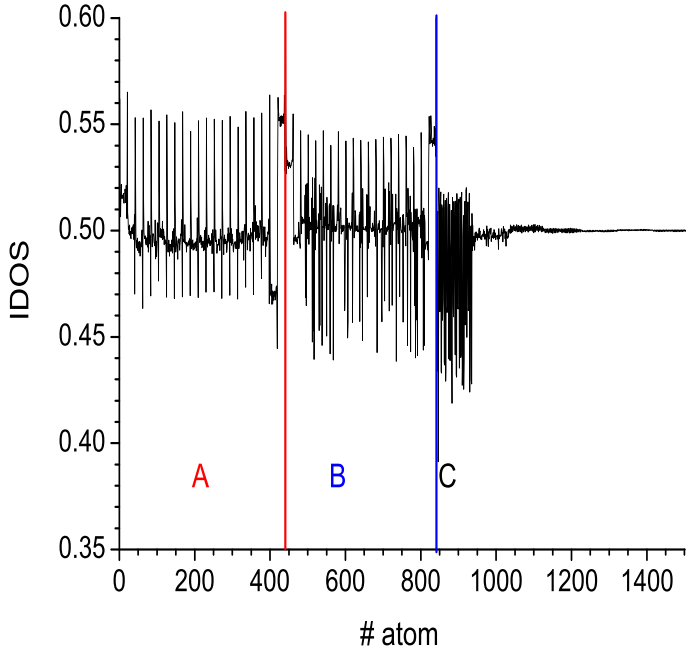


Figure 1. Atom projected integrated density of states per spin (IDOS) at the metal electrode (fcc-(1,1,1)) and the (24,24)-SWCNT. Labels A, B denote the two electrode interface-planes (with $21^2$ and $20^2$ atoms, respectively), whereas C denotes the carbon atom region (96 atoms at the interface unit cell). Note large fluctuations in the IDOS at the metal/SWCNT interface.

and diameter-dependent), whereas the most frequently used metal electrodes may have either a bigger WF than that (Au, Pd and Fe, Co, Ni 3d-transition metals) or a smaller one (e.g. Ti) [19]. The former typically results in transferring charge from the CNT to the electrode, whereas the latter { the other way round. As it follows from Fig. 1, the model under consideration here mimics the former case, with a noticeable electron de cit at the CNT interface.

The Green function of the extended molecule ($G_C$), as well as the density matrix ($\hat{n}$) and the conductance per spin ($G$) are de ned in a standard way as

$$G_C = (E \quad H_C \quad {}_L \quad {}_R)^{1}; \tag{2}$$

$$\hat{n} = \frac{1}{2}^{Z} \quad dE\, G_C\, (f_L \; {}_L + f_R \; {}_R)\, G_C{}^{y}; \tag{3}$$

$$G = \frac{e^2}{h} Tr^{n} \; {}_L G_C \; {}_R G_C{}^{y}{}^{o}; \tag{4}$$

where the respective subscripts C, L and R refer to the extended molecule (central part) and the left and right electrodes. In contrast to rather common wide-band type approximations, the present method is based on self-energies ( matrices) which are energy-dependent and have been expressed in terms of recursively computed surface Green functions $g(E)$ of in nite leads (electrodes) as well as the extended-molecule/electrode coupling matrices $V$:

$$= V g V^{y}: \tag{5}$$

The other quantities in Eq. (3) are the line-width (or broadening) matrices $= i( \quad {}^{y})$ and the Fermi-Dirac distribution functions $f$ , with $= L;R$.

## 3. Giant magnetoresistance in ferromagnetically contacted carbon nanotubes

Since the pioneering paper on the GMR e ect in CNT-based devices was published [4], there has been a lot of interest in electrical transport through ferromagnetically contacted nanotubes. It is now clear that the spin di usion length in nanotubes is quite long, and often exceeds a separation length between source and drain electrodes, which is routinely made as short as a few hundred nm nowadays. This means that the CNT may be quite attractive for spintronic application either as interconnects or active elements. So far most of GMR experiments on CNTs have been performed on relatively high resistive devices [4, 20, 21], corresponding to the tunnelling regime with resistance ($R$) of the order of M . Notably, quite recently the Basel group [22, 23] succeeded in fabricating devices whose resistance was substantially decreased down to the order of quantum resistance ($h/e^2 = 26{:}8$ k ). It is well-known from independent studies of

the Stanford [24] and Basel [25] groups that Pd makes excellent contacts with CNTs. The above-mentioned new highly transparent ferromagnetic contacts do also contain palladium ($Pd_{0.3}Ni_{0.7}$ alloy). In what follows, we calculate the giant magnetoresistance, defined (in a "pessimistic way") as

$$GMR = (G_{\uparrow,\uparrow} - G_{\uparrow,\downarrow})/G_{\uparrow,\uparrow}; \tag{6}$$

where the arrows denote the aligned and anti-aligned magnetizations of the metal electrodes, with G defined by Eq. 4. A system under consideration is an (8,8)-SWCNT both disorder-free and disordered. The Anderson type disorder is introduced by randomizing carbon on-site potentials and letting them vary in an interval [-W/2, W/2], where the disorder parameter W is set to 0.2t. This simple approach is intended to test whether or not in the case of GMR, a multiwall CNT can effectively be treated as equivalent to just its outer shall subjected to some perturbation from the inner shells. This hypothesis is generally believed to be acceptable by both theorists [26, 27] and experimentalists [28, 29]. Figure 2 shows how the GMR effect gets modified under the influence of Anderson-disorder. The obvious observations are that disorder destroys periodicity of GMR and decreases its absolute value from roughly 20% ([17],[18]) down to a few percent simultaneously reducing tendency of GMR to become negative. All these features are in accord with experimental data on GMR in multiwall carbon nanotubes (MWCNTs) with transparent ferromagnetic contacts [22, 23]. The most notable effect of the disorder is removing of the characteristic energy scale ( E ) in the conductance

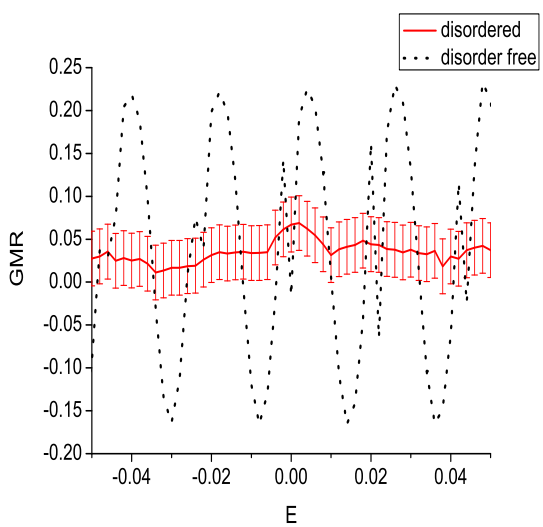


Figure 2. GMR of an (8,8) single-wall CNT ca 30 nm long, for the disorder-free (dotted curve) and disordered (solid line) cases. The latter is computed from the disorder-averaged conductances (over 100 random configurations), standard-deviation error bars are also shown. The presented energy range is close to the charge neutrality point (E = 0), with the hopping integral chosen as the energy unit (|t| = 2.7 eV).

spectrum. In the quasi-ballistic regime $E$ is related with energy-level spacings, and scales inversely proportional to the CNT length (see e.g. [30]). For less transparent contacts $E$ must be completed with a charging energy, i.e. the so-called addition energy is to replace the $E$ parameter. The double-peak structure visible in Fig. 2 (dotted curve) results from lifting of the spin degeneracy by the ferromagnetic electrodes. The splitting effect is however too subtle to be visible in the presence of disorder (solid curve).

## 4. Nanotubes in parallel and perpendicular magnetic fields

As regards a parallel (axial) field configuration, it was predicted theoretically that magnetic field can drastically change electronic band structure of carbon nanotubes [7, 9]. This may lead to opening of the energy gap in an initially metallic CNT and turn it into a semiconducting one. The same applies to a semiconducting CNT, which may reveal a more and more reduced gap with increasing magnetic field, and eventually become metallic. Recently, two important experimental papers have been published, that fully confirm aforementioned scenarios. The first one [31] visualizes in a direct way magnetic flux modulation of the energy gap in high-diameter MWCNTs, with an outer radius of about 15 nm which makes it possible to get the magnetic flux quantum $_0 = h/e$ at accessible fields of $B \quad 6T$. The AB effect can also be detected in much thinner single-wall carbon nanotubes, typically a few nm in diameter, although in this case obviously just a small part of the AB phase comes into play, nevertheless it is detectable by means of magneto-optical techniques under pulsed magnetic fields [32]. In this section we generalize the hitherto existing theoretical studies restricted to free CNTs, by taking into account the presence of electrodes and thereby on the one hand, the accompanying charge transfer, and on the other hand – the energy level broadening which becomes quite crucial for ultra short CNTs with transparent contacts. Incidentally, the charge transfer problem is seldom addressed in theoretical papers devoted to magnetoresistance problems, as it requires integration over all occupied states and makes calculations extremely computer-time consuming and expensive. Therefore theoreticians often skip the charge transfer issue and restrict themselves only to conductance calculations, which may be carried out just at the Fermi energy (or within a narrow "transport energy window"). The present studies go beyond this limitation.

We use the well-known Peierls substitution [9]

$$t \;\; ! \;\; t \exp[i2 \;\; '= \;\; _0]: \tag{7}$$

The factor $'$ is defined in terms of a magnetic $_p$ux $= B \; \frac{C_h}{2})^2$ penetrating a cross-section of the (m,n) CNT with perimeter $C_h = a \; \sqrt{n^2 + m^2 + mn}$, where $B$ stands for a uniform static magnetic field and the graphene lattice constant $a = 2{:}49$A is a length

unit of the theory

$$, = \begin{cases} \dfrac{x}{C_h} \; ; & \text{parallel field} \\ \dfrac{C_h}{2}\left[\dfrac{{}^{2}B \quad y}{x}\right]\cos\dfrac{2 \quad x}{C_h} \quad \cos\dfrac{2 \quad (x+ \quad x)}{C_h} \; ; & \text{perpendicular field.} \end{cases} \tag{8}$$

Circumferential and axial coordinates of carbon atoms are $x$, $x+ \quad x$, and $y$, $y+ \quad y$, respectively. It is noteworthy that within the present approach magnetic field enters not only off-diagonal block-elements of the Hamiltonian (via the Peierls substitution) but also the diagonal ones through the Zeeman splitting, $\frac{1}{2}g \quad {}_B B$. The relevance of the Zeeman splitting in the AB effect is often underestimated, but theoretical results of [33] as well as measurements presented in [31] show that it can lead to fairly pronounced effects. In fact the Zeeman splitting is taken into account here not only within the CNT but also in metal leads, since in the case of small-size devices there is no way to apply magnetic field locally without interfering the electrodes. The Peierls substitution has not however been applied to contacts. The reason is that it could be hardly implemented in the present recursive calculation scheme of infinite electrodes. Fundamentally different geometries of the SWCNTs and contacts, as well as strong screening effects within the (metal) contacts justify additionally this approximation. Figure 3 shows Aharonov

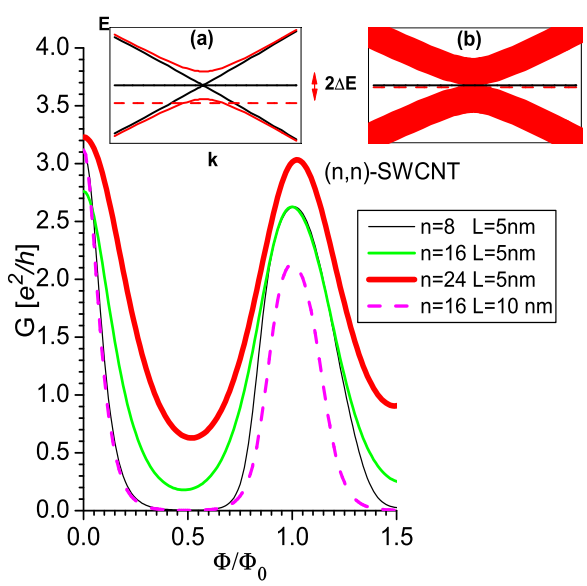


Figure 3. Magnetoconductance of small armchair SWCNTs in a parallel field vs magnetic flux. The inset (a) shows that when the doping is high the Fermi energy $E_F$ (dashed horizontal line) might lie outside the maximum magnetic field-induced energy gap, $2 \quad E = \quad |j|=n \quad g \quad {}_B B$, and the conductance never vanishes. In fact the same effect occurs for a much smaller $E_F$-shift provided the energy-level widths, originating from a strong CNT-electrode coupling are broad enough (Inset (b)).

Bohm oscillations in selected (n,n)-SWCNTs contacted to the model paramagnetic fcc-(1,1,1) electrodes. It is shown that conductance is a quasi-periodic function of with a period equal to $_0$. Remarkably, in general the conductance does not drop to zero at = $_0$=2. This might have been due to the fact that there is some charge transfer in the system which locates the Fermi energy beyond a magnetic eld-induced energy gap (see the inset a). In fact however it results from the calculations that the accompanying energy shift is by far smaller than half the magnetic eld-induced energy-gap. To understand the situation it must be realized that in devices with transparent contacts energy levels are quite broad. A zero- eld energy level spacing E is strongly dependent on nanotube axial length (L). In the ballistic regime E = $\sqrt{3}$ jtja=(2L) and the energy level broadening also scales as 1=L [30]. Thus for small-size nanotubes studied in this section with L 20a { 40a, the energy-level width turns out to be comparable with the energy-gap E . These two energy scales are close to each other because of comparable magnitudes of the perimeter (sampled with the axial eld) and the length. So a crucial role should be ascribe to the interplay between the energy-level broadening e ect and the magnetic eld-induced energy gap whose maximum value is proportional to the inverse nanotube radius. Consequently, as shown in Fig. 3 the AB e ect is very strongly dependent on the nanotube perimeter as far as the collapse of metal-semiconductor switching ability is concerned. The crossover takes place at the

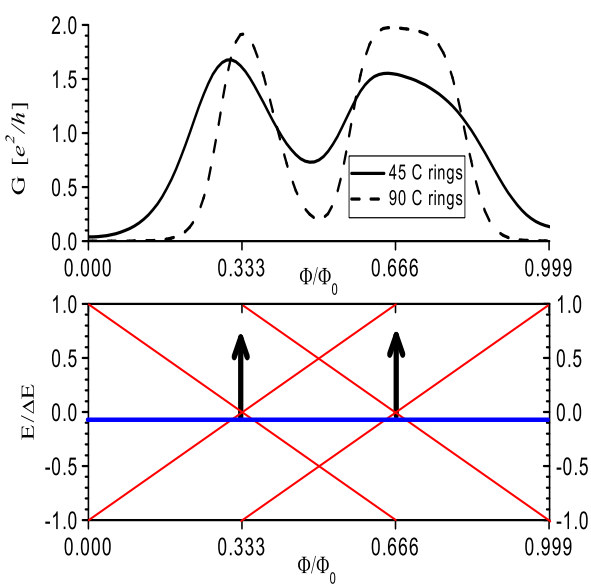


Figure 4. Top panel: Conductance of a (14,0)-SWCNT ca 5 nm (solid line) and 10 nm (dashed line) long vs. dimensionless magnetic ux. Bottom panel: Sketch for closing and opening of the energy gap (2 E), according to the AA theory. Vertical arrows indicate anticipated conductance peaks. The comparison of the panels shows clearly that energy levels are considerably broadened in electrically contacted nanotubes.

circumference-to-length ratio close to unity. This is clearly visible for the SWCNTs with n = 16 (perimeter $C_h$ = 7nm), which still have a considerable conductance at $= {}_0 = 0.5$ for L = 5 nm (middle curve), but not for L = 10 nm (dashed curve). It implies that if assumptions of the present theory were fulfilled then, e.g. a (150,150) CNT would lose its magneto-electrical switching efficiency for a length below ca 65 nm.

If the CNTs in question are nominally semiconducting zigzag-type ones, then again a quasi-period of the conduction oscillations is ${}_0$, but depending on the degree of doping, the nanotube perimeter (which determines the number of sub-bands and the maximum energy-gap, $2\ E = 2\ |t|=(\sqrt{3}\ n)$) as well as the length (responsible for the number of energy levels within a sub-band), one gets 2- and 3-peak conductance curves. In principle, the peak positions might be explained in terms of the Ajiki-Ando theory [7] and the aforementioned arguments about the interplay between the doping, the energy gap-width and the energy-level broadening. It results from Fig. 4 that deviations from the AA theory are large for short-length CNTs, and they manifest themselves by broadening of conductance peaks and disappearance of a conductance gap at $= {}_0 = 0.5$. Incidentally a noticeable asymmetry in the conductance peak-widths in Fig. 4 results from the Zeeman splitting which increases with the magnetic field. A pictorial, rather crude explanation of the results in terms of the AA theory is sketched

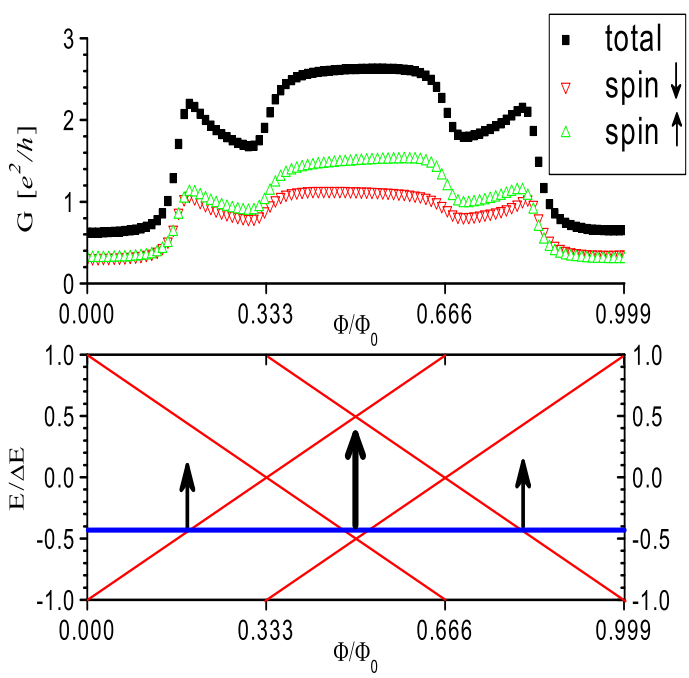


Figure 5. Same as Fig. 4 but for a (28,0)-SWCNT. The lower panel represents a possible interpretation of the upper one within the AA theory. In fact however the Fermi energy is always very close to E = 0, but the energy level widths are of the order of E = 2 for ultra short devices (cf Inset (b) in Fig. 3).

in the bottom panels of Figs. 4 and 5. The slanting lines over there represent the lowest energy level evolution as a function of magnetic ux (no Zeeman splitting is shown for clarity). Ideally the CNTs remain semiconducting except at the crossing points, where the energy gap gets closed. Indeed some traces of such a behavior are really displayed by these two gures. However the $E_F$-shift, as depicted in Fig. 5 (bottom horizontal line) is unrealistically large and inconsistent with the numerical results. As a matter of fact the actual $E_F$-shift is by more than one order of magnitude smaller than that (about 20 times), nevertheless the energy gaps get closed due to exceptionally broad energy level-widths occurring in these small-size devices having perimeters comparable with a length. Actually the AA theory in its conventional version applies to perfect, in nite CNTs of arbitrary chirality. It is however restricted to a low energy region in the energy spectrum ("light-cone" approximation) and disregards external contacts and any possible charging e ects. Nevertheless our results show that there are reminiscences of major AA features even under more complicated conditions than those originally assumed. It is interesting to note that the conductance spectra are spin-dependent due to the Zeeman splitting (up-triangles and down-triangles in Fig. 5) for high enough ( $_0$=6). This suggests that in the quasi-ballistic regime a spin polarization of the current owing through the CNT appears to be controllable by the magnetic eld strength.

Turning now to the perpendicular eld, we focused our attention on the armchair SWCNTs (5 nm long) and the (28,0)-zigzag one which have been studied above for the axial geometry. Figure 6 shows magnetic eld – conductance dependence of these nanotubes.

Remarkable features of the plot are that the conductances reveal oscillations with a decreasing amplitude and asymptotically approach the upper theoretical limit of $4e^2/h$ at huge elds. These features can be accounted for by the fact that energy bands get narrower and narrower as B increases (magnetic length $l_m = \sqrt{\ _0/(2\ B)}$ decreases), and eventually form Landau-like levels, with a decreasing but always nite width. It was shown in [34, 35] that interface conditions as well as charges in a nanotube length can bring an armchair nanotube to or out of the so-called on-resonance state with a conductance peak at the Fermi level (nota bene the o -resonance state has a conductance dip at $E_F$). Experimentally such a tuning is realized more conveniently by means of a gate voltage. As regards the magnetic eld, it spoils the on-resonance conductance and improves the o -resonance one. It was veri ed that indeed, there is such a competition responsible for the behavior of the magneto-conductance curves depicted in Fig. 6 for n = m = 16 and 24, respectively. The rst peak is due to promoting the Zeeman-split #-spin electron conductance from the o -resonance type at B = 0 to the on-resonance type at the rst peak position, and roughly the opposite process in the case of "-spin electrons (see the inset). It turns out that the former process prevails leading to a slightly negative magnetoresistance (positive magnetoconductance). For n = 8 in turn, initially the spin-dependent conductances give compensating contributions, resulting in nearly constant net conductance (up to 0.01). It should be stressed that the

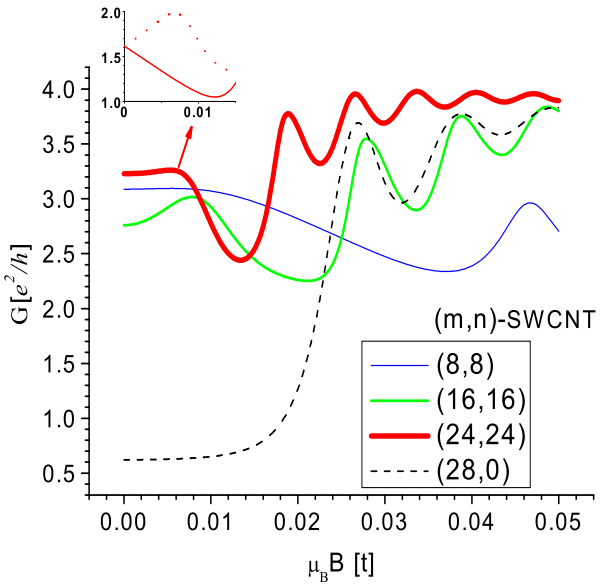


Figure 6. Magnetoconductance of (m,n)-SWCNTs at a perpendicular magnetic field. Note that quasi-periods of the curves scale inversely proportional with the CNT diameter, and G tends to $4e^2/h$. The inset shows spin-dependent contributions to the total conductance for m = n = 24 (G # – dotted line, G " – solid line).

described magnetoresistance mechanism develops within the quasi-ballistic regime in impurity-free systems. The effects described above are weaker and of another field-scale than the well-known interference phenomena, i.e. weak-localization (WL) and universal quantum fluctuations (UCF) [28, 29], and obviously the physics standing behind them is completely different. Experimentally the WL contribution can be identified on the basis of its temperature-dependence, and the UCF one may be effectively suppressed upon gate voltage-averaging of the conductance [29]. So in the case of the simultaneous presence of the interference phenomena and the ballistic magnetoresistance described above, the latter seems separable from the former ones.

Another point which needs commenting on is related with the fact that the present calculations are restricted to thin nanotubes (with diameters up to 33 A). In the parallel field the AB oscillations have a well-defined periodicity ($_0$) independently of the thickness, so the present findings could be applicable in a rather straightforward way to thick MWCNTs. In particular, the Aharonov-Bohm smearing, at the circumference-to-length ratio close to unity, shown here to be the inherent property of SWCNTs, should be detectable e.g. in a (150, 150) CNT system (most probably even in the Coulomb-blockade regime, see [31]) upon improving contact transparency and introduction of two buckles ca 20 nm away from each other.

The situation is more cumbersome for the perpendicular geometry, where, as seen in Fig. 6, the G(B) curves depend critically on the thicknesses involved, and there

is no way to make a pseudo-universal plot (replacing $_B B$ by a magnetic strength parameter $= R=l_m$ with a radius $R = C_h=(2\ )$ does not help at all). However it results from Fig. 6 that the rst magnetoresistance peak roughly appears within the interval $1 < < 2$, i.e. whenever the lowest Landau level emerges. So it is reasonable to anticipate that this trend will also be present in the case of thick CNTs if the aforemention conditions (ballisticity and transparency) are fulled. So the expected critical magnetic eld at which magnetoresistance changes its sign would be, e.g. 6 – 12 T for a (150,150)-CNT with a diameter 200A. Another argument in support to the suggestion that magneto-conductance in perpendicular magnetic elds is directly related with the Landau quantization is a nding that asymptotically for large B, conductance is no longer chirality-dependent and its behavior is totally determined by a nanotube diameter. For instance the (16,16)-SWCNT curve of Fig. 6 closely resembles that for a (28,0)-SWCNT (dashed curve) with practically the same diameter, for strong enough $_B B$. This means that magnetic eld localizes electron wave-functions making thereby circumferential boundary conditions irrelevant (cf [8]).

## 5. Summary and conclusions

In this study the attention has been focused on a quasi-ballistic spin-dependent transport through carbon nanotubes contacted to two external electrodes. Unlike some other authors, we use neither seamless electrodes (made also of CNTs) nor the so-called wide-band approximation. Moreover, while studying magnetic- eld dependence of the conductance we have included the Zeeman splitting not only in the CNT alone but also in the electrodes. So we have been in a position to take into account possible charge transfer and spin-polarization e ects, and estimate their combined impact on the ballistic magnetoconductance.

The relevance of the spin-degree of freedom is demonstrated by taking into account the following cases: (i) CNT sandwiched between ferromagnetic contacts, and (ii) nanotubes of various thickness, length and chirality placed in external magnetic eld oriented either parallel or perpendicular to the tube axis. In the former, it was shown that the GMR e ect in single-wall disorder-free CNTs may be quite large, exceeding 20% or so. The GMR is a quasi-periodic function of energy (controllable with a gate voltage) with a period related to a characteristic energy-scale for the problem at hand, namely the inter energy-level distance in the ballistic regime (and by analogy the addition energy in the Coulomb blockade case). Interestingly, as a function of energy the GMR may be both positive and negative (inverse GMR) with roughly the same absolute value. Upon introducing disorder, the situation substantially changes. Not only the amplitude of GMR decreases down to several percent but also its oscillations become aperiodic and the inverse GMR is in practice no longer present, at least in the vicinity of the charge neutrality point. Once such features have been recently established experimentally on MWCNT with transparent ferromagnetic contacts, it seems that single-wall CNTs with

disorder may really mimic behavior of multiwall CNTs. Putting it in other words, the present results give credit to the wide spread view that MWCNT transport properties can be regarded just as due to its outermost shell disturbed electrostatically by inner shells (assuming that the latter are out of contact to the leads).

As regards the in uence of a magnetic eld, it has been shown here that interface conditions, responsible for energy level widths and the charge transfer, modify the magnetoconductance spectra for parallel orientation without changing the period of the Aharonov-Bohm oscillations. In particular, if the charge transfer shifted $E_F$ happens to touch the closest energy-gap edge (considerably broadened by the strong coupling to the electrodes) then the conductance of arm chair CNTs remains nite even at $= {}_0/2$. For the same reason nominally semiconducting CNTs may have suppressed but nite conductance at $= 0$ and ${}_0$. Moreover the conductance reveals two- and three-peak structures which have been interpreted here as being reminiscent features of the Ajiki-Ando theory when either a large energy-level broadening or a high doping come into play. It is noteworthy that SWCNTs lose their ability to serve as magneto-electrical switches when their length-to-perimeter ratio approaches unity.

The magnetoconductance spectra of CNTs at a perpendicular eld, in turn, reveal pronounced oscillations having a pseudo-period which scales with a CNT radius. It has been found that in the (quasi) ballistic regime the magnetoresistance changes its sign at elds related to the onset of the rst Landau level. A clear dying down of magnetoconduction oscillations at the charge neutrality point (of the extended molecule) with the increasing magnetic eld is due to narrowing of the lowest Landau level-width.

## Acknowledgments

I thank the EU grant CARDEQ under contract IST-021285-2, and the Poznan Supercomputing and Networking Center for the computing time.

## References

[1] Baibich M N, Broto J M, Fert A, Nguyen Van Dau F, Petro F, Eitenne P, Creuzet G, Friederich A and Chazelas J 1988 Phys. Rev. Lett. 61 2472
[2] Tanaka M and Higo Y 2001 Phys. Rev. Lett. 87 026602
[3] Xiong Z H, Wu Di, Vardeny Z V and Shi J 2004 Nature 427 824
[4] Tsukagoshi K, Alphenaar B W and Ago H, 1999 Nature 401 572
[5] Zutic I, Fabian J and Sarma S D 2004 Rev. Mod. Phys. 76 323
[6] Sanvito S, 2004 Handbook of Computational Nanotechnology, American Science Publishers, California; cond-mat/0505134
[7] Ajiki H and Ando T 1993 J. Phys. Soc. Jpn. 62 1255
[8] Ando T 2005 J. Phys. Soc. Jpn. 74 777
[9] Saito R, Dresselhaus M S and Dresselhaus G, 1998 Physical Properties of Carbon Nanotubes, Imperial College Press
[10] Smit R H M, Noat Y, Untiedt C, Lang N D, van Hemert M C and van Ruitenbeek J M 2002 Nature 419 906

[11] Pasupathy A N, Bialczak R C, Martinek J, Grose J E, Donev L A K, McEuen P L and Ralph D C 2004 Science 306 86
[12] Postma H W Ch, Teepen T, Yao Z, Grifoni M, Dekker C 2001 Science 293 76
[13] Liang W J, Bockrath M, Bozovic D, Hafner J H, Tinkham M and Park H 2001 Nature 411 665
[14] Krompiewski S, Martinek J and Barnas J 2002 Phys. Rev. B 66 073412
[15] Frank S, Poncharal P, Wang Z L, de Heer W A, 1998 Science 280 1744
[16] Li H J, Lu W G, Li J J, Bai X D and Gu C Z 2005 Phys. Rev. Lett. 95 86601
[17] Mehrez H, Taylor J, Guo H, Wang J, Loland C 2000 Phys. Rev. Lett. 84 2682
[18] Krompiewski S 2005 physica status solidi (b) 242 226
[19] Xue Y and Rattner M 2003 Appl. Phys. Lett. 83 2429
[20] Zhao N, Monch I, Muhl T and Schneider C M 2002 Appl. Phys. Lett. 80 3144
[21] Kim J-R, So H M and Kim J-J 2002 Phys. Rev. B 66 233401
[22] Sahoo S, Kontas T, Schonenberger C and Surgers C 2005 Appl. Phys. Lett. 86 112109
[23] Sahoo S, Kontas T, Furer J, Hoffmann C, Graber M, Cottet A and Schonenberger C 2005 Nature Physics 1 99; cond-mat/0511078
[24] Javey A, Guo J, Wang Q, Lundstrom M and Dai H, 2003 Nature 424 654
[25] Babic B, Furer J, Iqbal M and Schonenberger C, 2004 in Electronic Properties of Synthetic Nanostructures, AIP Conf. Proc. 723, 574; cond-mat/0406626
[26] Egger R and Gogolin A O 2001 Phys. Rev. Lett. 87 066401
[27] Triozon F, Roche S, Rubio A and Mayou D 2004 Phys. Rev. B 69, 121410
[28] Bachtold A, Strunk C, Salvetat J-P, Bonard J-M, Forro L, Nussbaumer T and Schonenberger C 1999 Nature 397 673
[29] Stojetz B, Miko C, Ferro L. and Strunk C 2005 Phys Rev. Lett. 94 186802
[30] Krompiewski S, Nemec N, Cuniberti G 2006 physica status solidi (b) 243 179
[31] Coskun U C, Wei T-C, Vishveshwara S, Goldbart P M and Bezryadin A 2004 Science 304 1132
[32] Zaric S, Ostolic G N, Kono J, Shaver J, Moore V C, Strano M S, Hauge R H, Smalley R E and Wei X 2004 Science 304 1129
[33] Jiang J, Dong J and Xing D Y 2000 Phys Rev. B 62 13209
[34] Krompiewski S 2003 physica status solidi (b) 196 29
[35] Krompiewski S 2004 J. Magn. Magn. Mat. 272 1645